L_p-Norm-Based Sparse Regularization Model for License Plate Deblurring

CHENPING ZHAO [1,2], YINGJUN WANG[3], HONGWEI JIAO[1], JINGBEN YIN[1], AND XUEZHI LI[2]

[1]School of Mathematical Science, Henan Institute of Science and Technology, Xinxiang 453003, China
[2]College of Mathematics and Information Science, Henan Normal University, Xinxiang 453007, China
[3]School of Information Engineering, Henan Institute of Science and Technology, Xinxiang 453003, China

Corresponding author: Chenping Zhao (zcp0378@163.com)

ABSTRACT We propose an L_p-norm-based sparse regularization model for license plate deblurring, which is motivated by distinctive properties of license plate images. For the blurred images, general deblurring methods may restore a good overall visual effect. However, in real-life traffic surveillance system, the deblurring results may be not good for license plates. The main reason lies in that general deblurring methods do not give sufficient thought to the features of license plate, which could be important priors for deblurring. Focusing on this issue, analysis on the statistical distribution characteristics of the license plates are launched, based on which an L_p-norm-based regularization model is proposed. Furthermore, alternating direction method of multipliers are introduced to solve the model. Experimental results demonstrate that the proposed model performs favorably against the state-of-the-art license plate image deblurring methods.

INDEX TERMS License plate image, image deblurring, regularization model, alternating direction method of multipliers.

I. INTRODUCTION

With the increasing number of vehicles, traffic violations such as running the red light and hit-and-run increase rapidly. As a result, license plate recognition (LPR), a process that extract vehicle license plate information, has been greatly developed and utilized in numerous traffic-related problems [1]–[4]. Unfortunately, although the drive recorders or surveillance cameras perform much better than before, the license plates of vehicles are often blurred due to various reasons. As a result, this brings great challenges to LPR. Summarily speaking, license plate deblurring is very important in the traffic surveillance system.

There are several factors that give rise to the blurring corruption on the license plate images. The first factor is the surrounding environment. For example, the effects of illumination intensity, snow and fog, may increase the possibility of the blur. The second factor comes from the movements of the vehicle. For example, when the vehicles run a red light, they are often in a very fast speed, therefore, the captured images

are likely to be blurred. The third factor is the monitor system. For the scenario of static cameras, since that the surveillance cameras are often placed at higher positions, far away from the target vehicle, so the collected image is low-resolution, resulting in poor image quality. Moreover, the performance of the drive recorders is also an important factor. They can provide a wealth of information when an accident occurs, and the recorded information can be used as evidences [5]. However, the snapshots from a drive recorder also suffer from serious blur, especially when the relative speed of vehicles is high, the road surface is not flat, or the light field is low.

Focusing on license plate deblurring issue, a few license plate deblurring methods have been proposed [6]–[9]. Most of above methods developed based on the assumption that the images or videos only suffer from the low resolution or defocus blur, rather than motion blur and other blur. Under this assumption, the overall distribution of pixels' intensity do not change too much. However, when the license plates suffer motion blur or other type of blur, which would change the overall distribution of pixels' intensity, general recognition methods would fail in this situation. Authors in [10] proposed an L_0-regularized deblurring model for text image, based on

(a)Ground-truth   (b)Defocus blurring   (c)Motion blurring   (d)Defocus& Motion blurring

(e)Histogram of (a)   (f)Histogram of (b)   (g)Histogram of (c)   (h)Histogram of (d)

(i)Gradient of (a)   (j)Gradient of (b)   (k)Gradient of (c)   (l)Gradient of (d)
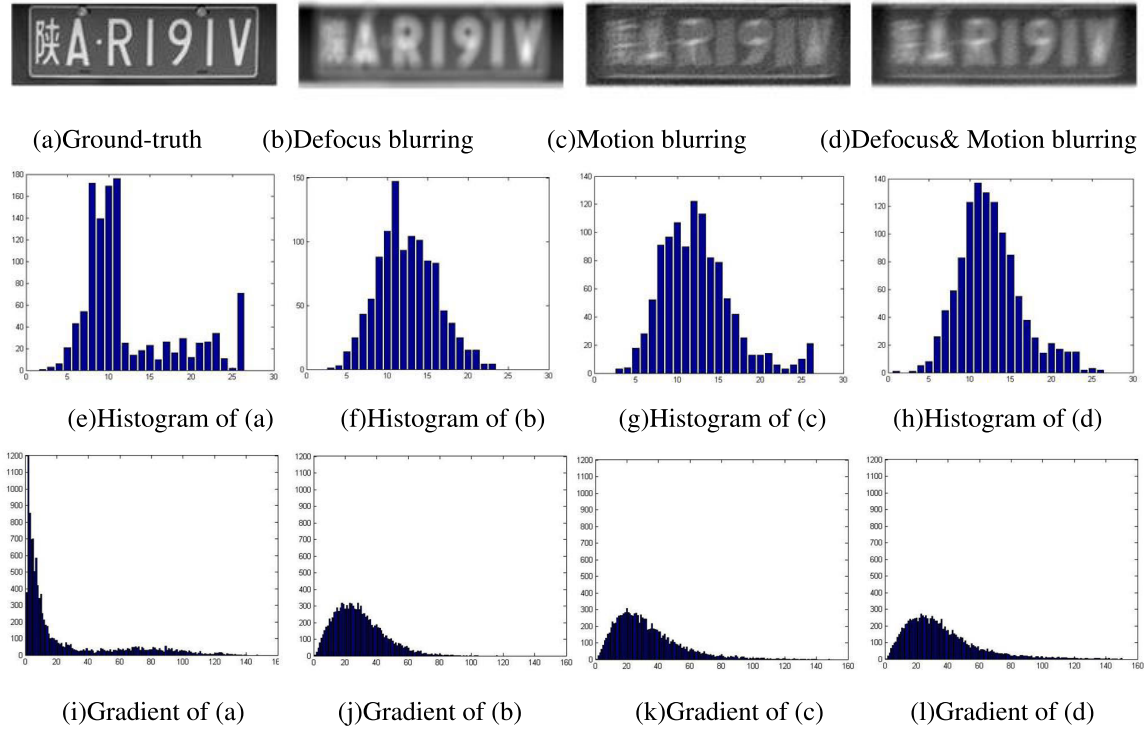
FIGURE 1. Influences of blurring on license plate image.

which, authors in [11] introduced L_0-norm based deblurring method into LPR process. However, the experimental results in Fig.1 indicate that L_0-norm can not best reflect the histogram of license plate images.

The aim of this paper is to recover license plates under the blurring corruption, especially the defocus blurring and the motion blurring. The statistical distribution characteristics of the license plates is first analyzed, based on which, a new deblurring method is proposed. Specifically, the major contributions of this paper are summarized as follows.

- We discuss on the statistical distributions of the license plates, and obtain the conclusion that the gradient histogram of the ground-truth approximately obey the Hyper-Laplacian distribution. With above consideration, we propose an L_p-norm-based regularization deblurring model.
- For the numerical scheme, we introduce the alternating direction method of multiplier algorithm to solve the propsed model, which can ensure the convergence and obtain the satisfying results.
- In the experiment section, we give detailed discussion on the key parameters, and analyze their effects on the deblurring performance.

The remainder of the paper is organized as follows. In Section 2, We propose new deblurring model, design the numerical algorithm and analyze the advantage of the proposed model. In Section 3, we present some experimental results obtained by our method and evaluate our method by both objective metrics and visual effects. We conclude

the paper and present some guidelines for future work in Section 4.

II. THE PROPOSED MODEL AND ALGORITHM
A. THE PROPOSED MODEL
The degradation problem of image blur is usually modeled as

$$f = Hu + n, \qquad (1)$$

where f is the degraded image, H is modeled as the blur kernel, n is the Gaussian noise and u is the desired ground-truth. Under the assumption that content and background regions have nearly uniform intensity values in text images, Authors of [10] suggested an L_0 regularization on the image intensity and its gradient, and proposed the deblurring model

$$\min_{u,H} \|Hu - f\|_2^2 + \lambda_1 \|u\|_0 + \lambda_2 \|\nabla u\|_0 + \gamma \|H\|_2^2. \qquad (2)$$

Based on (2), authors in [11] proposed a closed loop, in which an L_0-norm based deblurring method and a license plate recognition process are carried out alternatively.

Taking defocus blur and motion blur as examples, we analyze the features of license plate images and observe the influences of blurring on license plate images. The experimental results are shown in Fig.1, where (a) is the ground-truth, (b) is the defocus blurred license plate with the defocus blur kernel selected as Gaussian kernel with range 7×7, (c) is the motion blurred license plate with the motion blur kernel selected as a horizontal direction linear kernel with length $= 15$, and (d) is the degraded version with defocus blur and motion blur simultaneously existing. (e-h) are the intensity histograms of (a-d), respectively. (i-l) are the histograms of
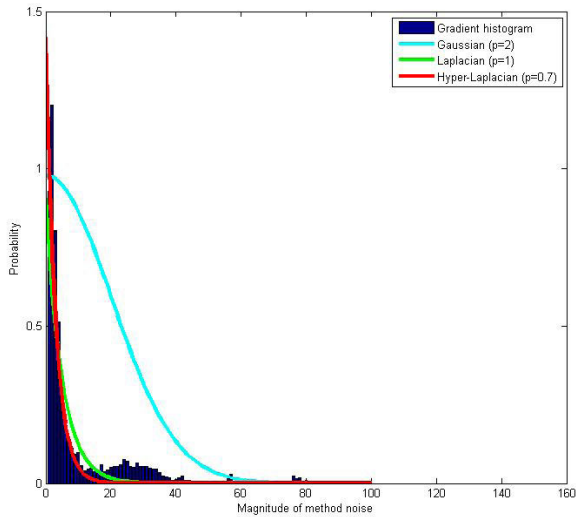
FIGURE 2. Distribution of the gradient histogram and the Gaussian, Laplacian, and Hyper-Laplacian distribution.

the gradient of (a-d), respectively. From the second row of Fig.1, it can be seen that the intensity histograms the blurred license plates perform slightly more uniform and smooth than that of the ground-truth, both with the defocus blur and the motion blur. However, since that the background of license plates is complex than the text, not just black and white anymore. As a result, the L_0-norm penalty on the image intensity in (2) is not suitable for license plate image deburring. In the third row of Fig.1, the gradient histogram of the ground-truth in Fig.1(i) performs sparsely. More precisely, it approximately obeys a Hyper-Laplacian distribution. The gradient histograms of the blurred license plate images in Fig.1 (j-l) are no longer sparse. They are much more uniform and smooth. So a sparse norm is desired to regularize the prior of the gradient.

In Fig.2, we plot the averaged gradient histogram of license plates, together with the Gaussian type, Laplace type and Hyper-Laplace type distribution. It is observed that the gradient histogram is more closely approximated to the Hyper-Laplace distribution.

Based on the above analysis, we introduce L_p norm into the deblurring method, and formulate the license plate deblurring model as

$$\min_{u,H} \|Hu - f\|_2^2 + \alpha \|\nabla u\|_p^p + \beta \|H\|_2^2. \quad (3)$$

where p is an important parameter, and was suggested to float in [0.5, 0.8] [12]. In this paper we first model the range of the parameter as $p \in [0, 1]$, then discuss its impact on the deblurring quality in the experimental section. Specifically, if p is selected as 0, problem (3) is similar with the deblurring model in [10], and if $p = 1$, $\|\nabla u\|_p^p$ degrades as the well-known total variation (TV) norm $\|\nabla u\|_1$.

B. NUMERICAL ALGORITHM
Taking advantage of the result in [13], we introduce the alternating direction method of multiplier (ADMM) algorithm to

---

Algorithm 1 Deblurring Algorithm for License Plate Images

Input: Choose a group of intial point $\{u^0, d^0, H^0, \lambda^0\}$, the proper parameters $\{p, \alpha, \beta, \mu\}$, and generate new iteration via the following scheme.

1: **for** $k = 1, 2, \cdots$, **do**
2: Update u:
3: $\quad u^{k+1} = \underset{u}{\operatorname{argmin}}\{\|H^k u - f\|_2^2 + \mu \|\nabla u - d^k + \lambda^k\|_2^2\}$
4: Update d:
5: $\quad d^{k+1} = \underset{d}{\operatorname{argmin}}\{\alpha \|d\|_p^p + \mu \|\nabla u^{k+1} - d + \lambda^k\|_2^2\}$
6: Update H:
7: $\quad H^{k+1} = \underset{H}{\operatorname{argmin}}\{\|Hu^{k+1} - f\|_2^2 + \beta \|H\|_2^2\}$
8: Update Lagrange multiplier λ:
9: $\quad \lambda^{k+1} = \lambda^k + (\nabla u^{k+1} - d^{k+1})$
10: end **for** if some stopping criterion is satisfied.

Output: Output u.

---

solve the minimization problem (3), To derive the ADMM algorithm for our model, we introduce a new variable and reformulate (3) as the following constrained minimization problem

$$\min_{u,d,H} \|Hu - f\|_2^2 + \alpha \|d\|_p^p + \beta \|H\|_2^2, \quad \text{s.t.} \quad d = \nabla u. \quad (4)$$

The corresponding augmented Lagrangian function is

$$L(u, d, H; \lambda) = \|Hu - f\|_2^2 + \alpha \|d\|_p^p + \beta \|H\|_2^2 \\ + \mu \|\nabla u - d + \lambda\|_2^2, \quad (5)$$

where λ is the scaled Lagrangian multiplier, and μ is the penalty parameter. The ADMM for (5) is shown as Algorithm 1.

In the following, we analyze the resulting sub-problems, and show that they can be easily handled with. In addition to the trivial task of updating the Lagrange multiplier λ, there are three main sub-problems at each iteration, and we will discuss them one by one.

- u-subproblem. The u-related subproblem is equivalent to

$$u^* = \underset{u}{\operatorname{argmin}} \left\{ \|Hu - f\|_2^2 + \mu \|\nabla u - d + \lambda\|_2^2 \right\}. \quad (6)$$

Since the objective function in (6) is differentiable, the closed-form solution can be calculated through the following formula.

$$u^* = \left(H^T H + \mu \nabla^T \nabla \right)^{-1} \left(H^T f + \mu \nabla^T (d - \lambda) \right) \\ = F^{-1} \left(\frac{\overline{F(H)} \circ F(f) + \mu F(\nabla^T (d - \lambda))}{\overline{F(H)} \circ F(H) + \mu F(\nabla^T \nabla)} \right), \quad (7)$$

where F denotes $2-$ dimension Fourier transform, F^{-1} denotes $2-$ dimension inverse Fourier transform, $\bar{a}$ denotes complex conjugate of a, "$\circ$" stands for the component-wise multiplication, and the division is operated component-wisely.
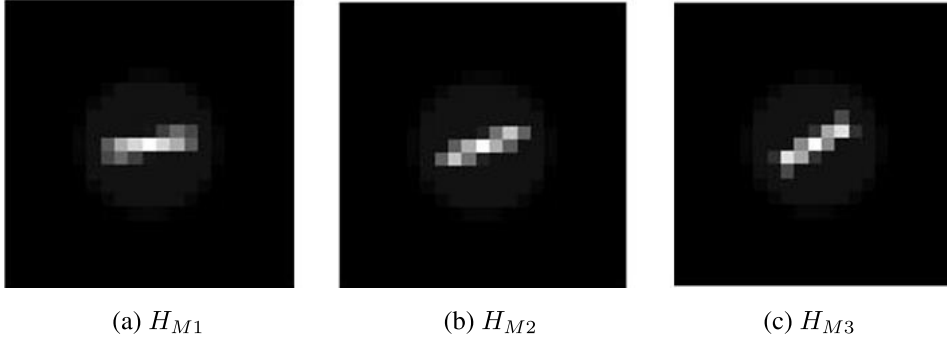
FIGURE 3. Some test license plate images.

FIGURE 4. Three mixed-blurring kernels.

Algorithm 2 Generalized Soft-Thresholding Operater $y = \text{GST}_s^p(x)$

Input: Given p, s, x, J, calculate $y = \text{GST}_s^p(x)$ as following process:

1:    if $|x| \leq \tau^p(x)$, then $y = 0$,
2:    if $|x| \geq \tau^p(x)$, we initialize $y^{(0)} = |x|$, and calculate y through the following iterative process:
3:      for $k = 1, 2, \cdots, J$
4:      $y^{k+1} = |x| - p \cdot s \cdot (y^{(k)})^{p-1}$,
5:      end
6:    $y = \text{sgn}(x) y^{(k)}$

Output: y

• d-subproblem. The d-related subproblem corresponds to the optimization problem

$$d^* = \underset{d}{\arg\min} \left\{ \alpha \|d\|_p^p + \mu \|\nabla u - d + \lambda\|_2^2 \right\}. \quad (8)$$

The problem is regarded as a generalized soft thresholding method in [12], and formularized as

$$d^* = \text{GST}_{\frac{\mu}{\alpha}}^p (\nabla u + \lambda), \quad (9)$$

where GST refers to the generalized soft-thresholding operator defined as in Algorithm 2. Noting that the iteration number in Algorithm 2 is empirically selected as $J = 2$ or 3, with which we can obtain satisfactory results.

• H-subproblem. The H-related subproblem amounts to solve

$$H^* = \underset{H}{\arg\min} \left\{ \|Hu - f\|_2^2 + \beta \|H\|_2^2 \right\}. \quad (10)$$

The closed-form solution for (10) is

$$H^* = F^{-1} \left(\frac{\overline{F(u)} \circ F(f)}{\overline{F(u)} \circ F(u) - \beta I} \right), \quad (11)$$

where I denotes identity operator.

C. ADVANTAGES OF OUR MODEL

It is noted that if $p = 1$, the problem in (3) degenerates into the TV-norm based deblurring method [14], [15], which tends to produce staircase effects during the deblurring process. If $p = 0$, deblurring model (3) degenerates into the L_0 regularized model [10]. It is known that the prior $\|x\|_0$ counts the number of nonzero-intensity pixels. However, if the image does not contain zero-gradient pixels, it always appears as $\|x\|_0 \equiv C$, where C is the total number of pixels in the license plate image and it is a constant. Therefore, the minimization problem would fall into a trivial solution.

Compared to the above two scenarios, the proposed model with $L_p(0 \leq p \leq 1)$-norm is more competitive. On the one hand, the regularization with $0 < p < 1$ can better describe the distribution of the gradient for the license plate image. Therefore, the proposed model can better restore the image edges and details, and obtain the better debluring results. On the other hand, our model can be regarded as the generalized form of the other two ones, which make the proposed method has more significance for promotion and application.

III. EXPERIMENTAL RESULTS AND ANALYSIS

In this section, several experimental results are reported to validate the proposed method. 389 images taken from the LP databases of [16]–[19] are tested, and six of which are displayed in Fig.3. Without loss of generality, we mainly report the experimental results under the mixture form of the defocus and motion blur. The defocus blur is selected as a circular averaging filter H_d with radius of 5. The motion blur consists of two causes: rotation unclock-wise through an angle θ (in degree) and shifting by L (in pixel). We consider $H_1 : (L, \theta) = (5, 15°)$, $H_2 : (L, \theta) = (5, 20°)$, and $H_3 : (L, \theta) = (5, 25°)$, respectively. Three mixed-blurring kernels of defocus and
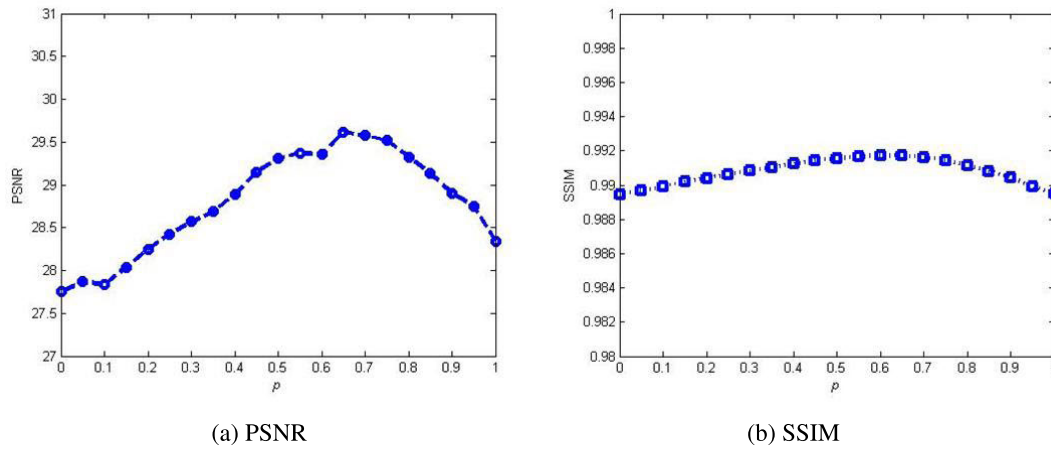
(a) PSNR   (b) SSIM

FIGURE 5. Plots of the indexes versus different values of parameter *p*: (a) is the variation tendency of PSNR, and (b) is the variation tendency of SSIM.

TABLE 1. Deblurring results with different *p*.

Image	Index	$p = 0.5$	$p = 0.6$	$p = 0.7$	$p = 0.8$
test1	PSNR/SSIM	29.38/0.9919	29.43/0.9922	29.58/0.9923	29.47/0.9920

(a)Blurred image   (b)$p = 0$: PSNR=27.51, SSIM=0.9842

(c)$p = 1$: PSNR=28.31, SSIM=0.9831   (d)$p = 0.7$: PSNR=29.37, SSIM=0.9948

FIGURE 6. Deblurring results with different *p*.
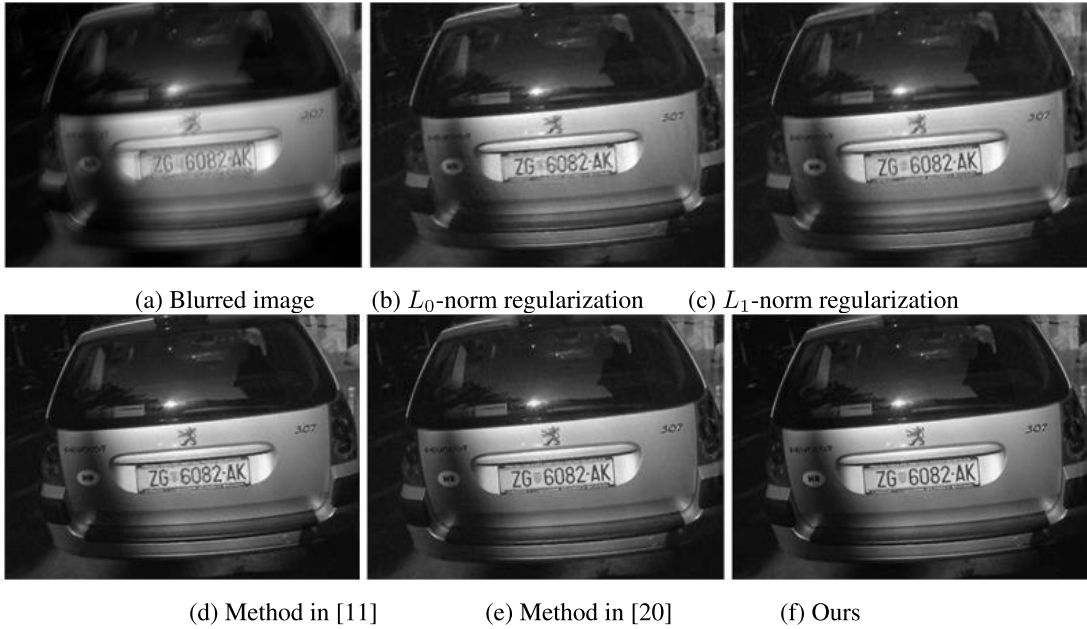
motion blur $H_{M1} = \frac{1}{2}(H_d + H_1)$, $H_{M2} = \frac{1}{2}(H_d + H_2)$, and $H_{M3} = \frac{1}{2}(H_d + H_3)$ are shown in Fig.4. Furthermore, we also add i.i.d. white Gaussian noise in the

simulation process to show the robustness of our method to noise.

We utilize the peak signal-to-noise ratio (PSNR) and the structure similarity index (SSIM) as performance measures,

TABLE 2. Deblurring performance of different methods for three mixed blur.

Blur	Image	Index	L_0	L_1	[11]	[20]	Ours
H_{M1}	test1	PSNR/SSIM	28.31/0.9877	28.62/0.9862	29.31/0.9922	29.56/0.9936	**30.12/0.9990**
	test2	PSNR/SSIM	28.51/0.9879	29.20/0.9865	29.42/0.9921	29.59/0.9940	**30.25/0.9989**
	test3	PSNR/SSIM	28.54/0.9883	29.41/0.9866	29.52/0.9926	29.78/0.9945	**30.41/0.9982**
	test4	PSNR/SSIM	28.16/0.9865	28.42/0.9867	28.89/0.9920	29.08/0.9941	**29.80/0.9979**
	test5	PSNR/SSIM	28.08/0.9862	28.07/0.9843	28.73/0.9917	28.87/0.9940	**29.41/0.9980**
	test6	PSNR/SSIM	28.04/0.9859	27.99/0.9846	28.40/0.9919	28.53/0.9939	**29.32/0.9976**
H_{M2}	test1	PSNR/SSIM	27.89/0.9856	28.74/0.9845	29.23/0.9920	29.32/0.9950	**29.92/0.9981**
	test2	PSNR/SSIM	28.13/0.9859	29.05/0.9847	29.25/0.9923	29.27/0.9949	**30.01/0.9982**
	test3	PSNR/SSIM	28.43/0.9861	29.16/0.9849	29.37/0.9925	29.48/0.9957	**30.11/0.9973**
	test4	PSNR/SSIM	27.95/0.9860	27.90/0.9848	28.55/0.9912	28.63/0.9951	**29.68/0.9968**
	test5	PSNR/SSIM	27.53/0.9852	27.85/0.9836	28.30/0.9914	28.39/0.9943	**28.89/0.9963**
	test6	PSNR/SSIM	27.36/0.9849	27.71/0.9838	28.21/0.9918	28.27/0.9940	**28.60/0.9959**
H_{M3}	test1	PSNR/SSIM	27.51/0.9842	28.31/0.9831	28.97/0.9906	29.01/0.9911	**29.57/0.9921**
	test2	PSNR/SSIM	27.96/0.9848	28.65/0.9838	29.20/0.9911	29.21/0.9936	**29.43/0.9951**
	test3	PSNR/SSIM	28.18/0.9850	28.96/0.9837	29.25/0.9913	29.27/0.9639	**29.54/0.9956**
	test4	PSNR/SSIM	27.59/0.9843	28.01/0.9826	28.56/0.9910	28.62/0.9926	**28.75/0.9954**
	test5	PSNR/SSIM	27.36/0.9832	27.96/0.9829	28.30/0.9911	28.41/0.9935	**28.36/0.9952**
	test6	PSNR/SSIM	27.29/0.9830	27.91/0.9820	28.01/0.9900	28.23/0.9925	**28.20/0.9949**

(a) Blurred image (b) L_0-norm regularization (c) L_1-norm regularization

(d) Method in [11] (e) Method in [20] (f) Ours

FIGURE 7. Deblurring results for H_{M1}.

which are respectively defined as

$$\text{PSNR} = 20\log_{10}\left(\frac{255n}{\|u - u_0\|_2}\right),$$

$$\text{SSIM} = \frac{2\mu_u\mu_{u_0}\left(2\sigma + c_2\right)}{\left(\mu_u^2 + \mu_{u_0}^2 + c_1\right)\left(\sigma_u^2 + \sigma_{u_0}^2 + c_2\right)}, \quad (12)$$

where u_0 is the original image, u is the restored image, μ_u and μ_{u_0} denote there means, σ_u^2 and $\sigma_{u_0}^2$ represent their variances, respectively. σ is the covariance of u and u_0, and $c_1 > 0$, $c_2 > 0$ are constants. For PSNR, a higher value implies better quality of the restored image. For SSIM, its value will be closer to 1 when the restored image more similar to the ground-truth.

In the following, we first discuss the parameter setting in Algorithm 1, especially the influence of the parameter p on the performance of the deblurring model. Then we report the experimental results of the proposed method and its comparison with the state-of-the-art methods.

A. CRITERIA OF CHOOSING PARAMETERS

To start up the deblurring algorithm, the parameter p, α, β and μ are needed to be given. p is model parameter, which will be particularly analyzed in the below paragraph. α and β are regularization parameters to keep balance among the terms in problem (3). Through a lot of experiments, the best parameter α can be chosen from the range [8, 10], and
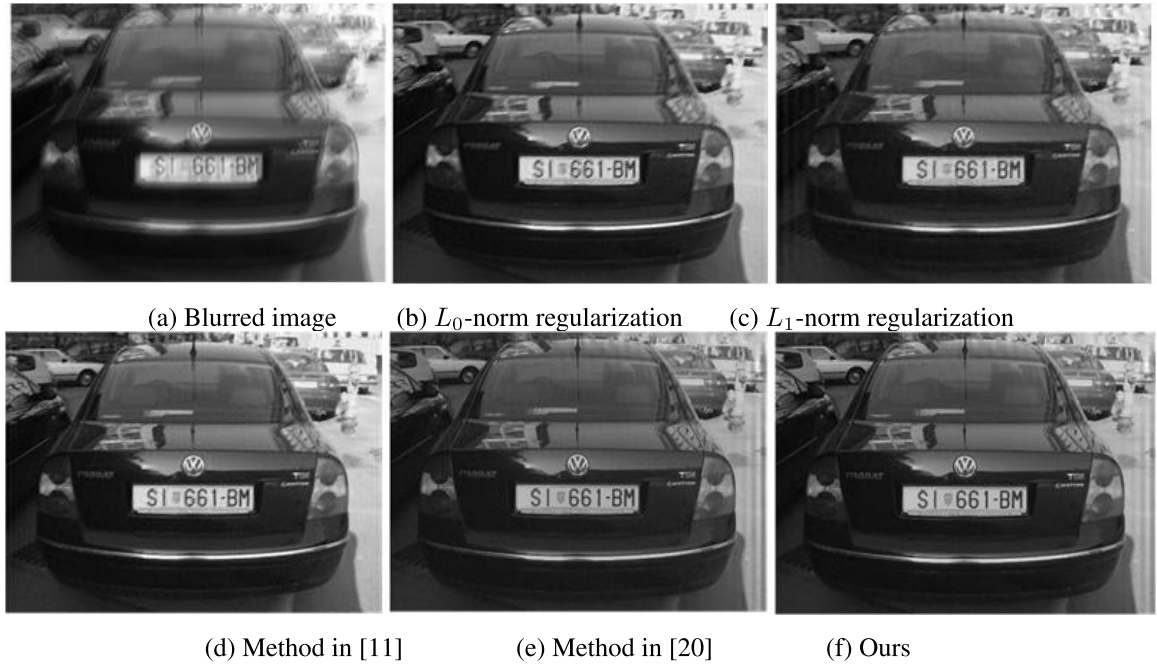
| (a) Blurred image | (b) L_0-norm regularization | (c) L_1-norm regularization |
| (d) Method in [11] | (e) Method in [20] | (f) Ours |

FIGURE 8. Deblurring results for H_{M1}.

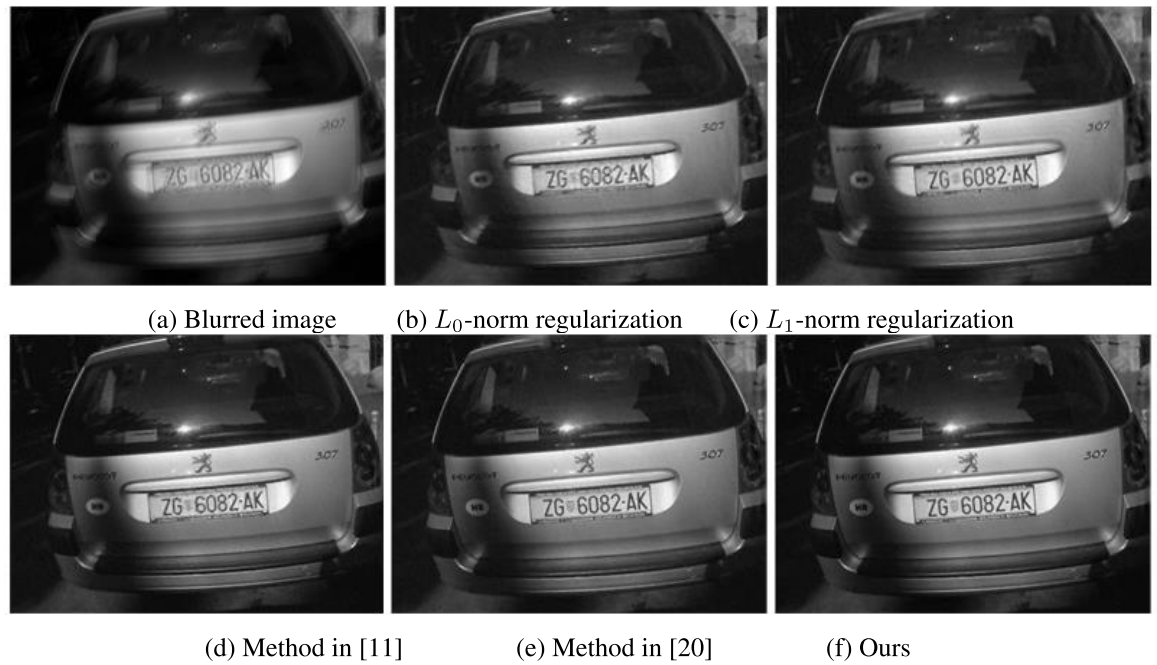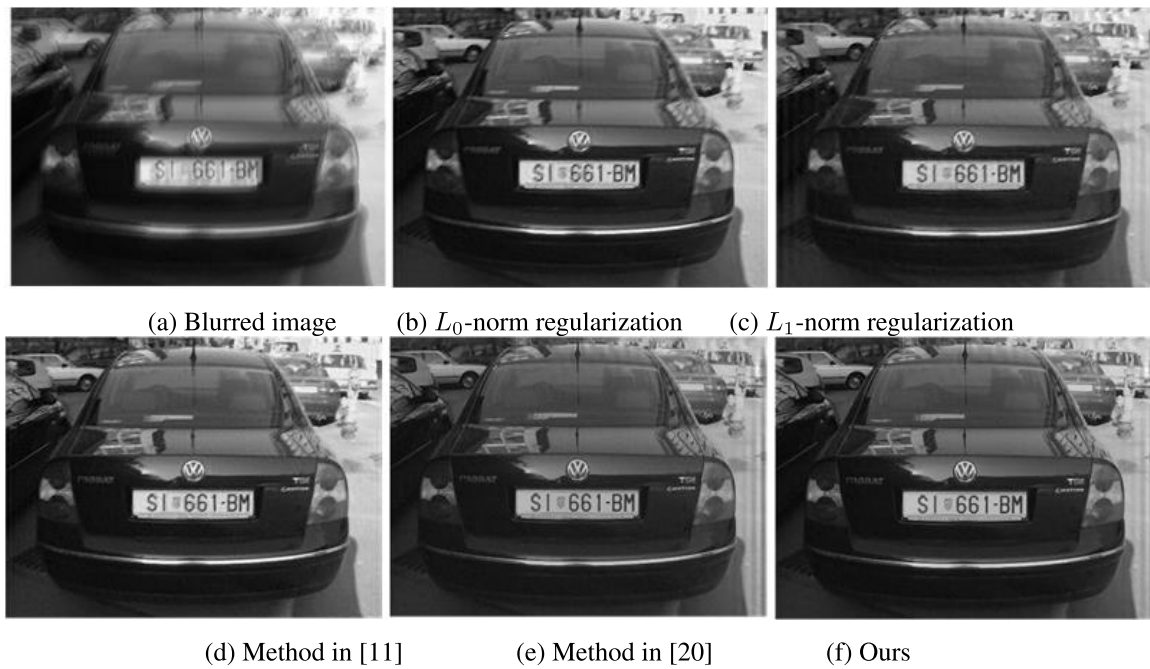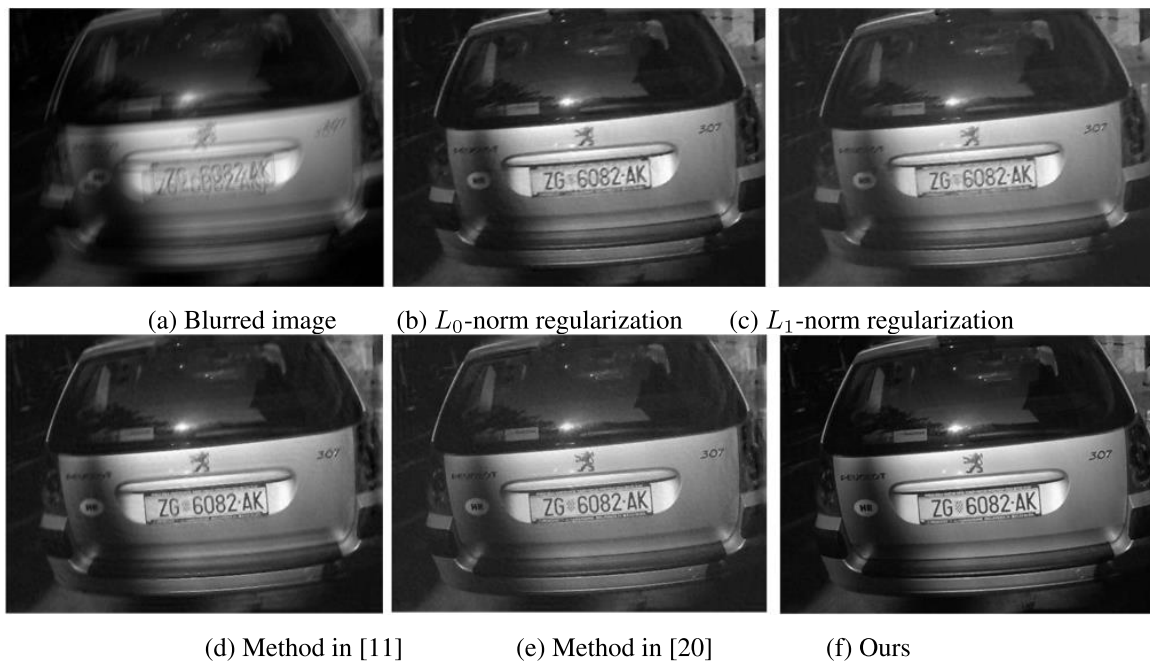| (a) Blurred image | (b) L_0-norm regularization | (c) L_1-norm regularization |
| (d) Method in [11] | (e) Method in [20] | (f) Ours |

FIGURE 9. Deblurring results for H_{M2}.

the best selection of β can be found from the range [2, 5]. μ is the penalty parameter in the ADMM scheme, which is empirically selected as 10.

Since p is an important parameter in the proposed model, we evaluate the deblurring effects with different p through experiments. We report the average PSNR and SSIM of the restored images in Fig.5. It is observed that the PSNR and SSIM are higher with $0 < p < 1$ than that $p = 0$ or $p = 1$. Especially, the best selection is among $p \in (0.5, 0.8)$.

In Fig.6, we display the visual results for the image "test1" with $p = 0$, $0 < p < 1$ ($p = 0.7$) and $p = 1$, and the corresponding PSNR and SSIM in the caption. It is clear that the visual result of $0 < p < 1$ ($p = 0.7$) outperforms other two cases. Furthermore, We unfold the PSNR/SSIM results with $p = 0.5, 0.6, 0.7, 0.8$ in Table.1. It can be found that the maximum value of both PSNR and SSIM are at the point $p = 0.7$. The variation ranges of both the two indexes are trivial, the former is no more than 0.2, and the latter no more

(a) Blurred image   (b) L_0-norm regularization   (c) L_1-norm regularization

(d) Method in [11]   (e) Method in [20]   (f) Ours

FIGURE 10. Deblurring results for H_{M2}.

(a) Blurred image   (b) L_0-norm regularization   (c) L_1-norm regularization

(d) Method in [11]   (e) Method in [20]   (f) Ours

FIGURE 11. Deblurring results for H_{M3}.

than 0.0004. Summarizing above results, it is reasonable to take $p = 0.7$ as the representative selection of the scenario $0 < p < 1$ in the following experimental tests.

B. COMPARISONS OF DEBLURRING RESULTS

We evaluate the performance of the proposed method, and compare it with state-of-the-art methods: the L_0-norm based regularization model, i.e. the work in [10], the L_1-norm based regularization model, the license plate deblurring method in [11] and the license plate deblurring method for fast moving vehicle in [20].

We first report the average PSNRs and SSIMs of the restored images by different methods in Table 2. The best results are in bold font. It can be observed that the PSNRs and SSIMs of the proposed method are superior than that of other several methods. Taking the results in Fig.9 as example, it is to remove the H_{M2} blur for the example ''test3''. In terms of PSNR, our method improves L_0-norm regularization,

(a) Blurred image   (b) L_0-norm regularization   (c) L_1-norm regularization

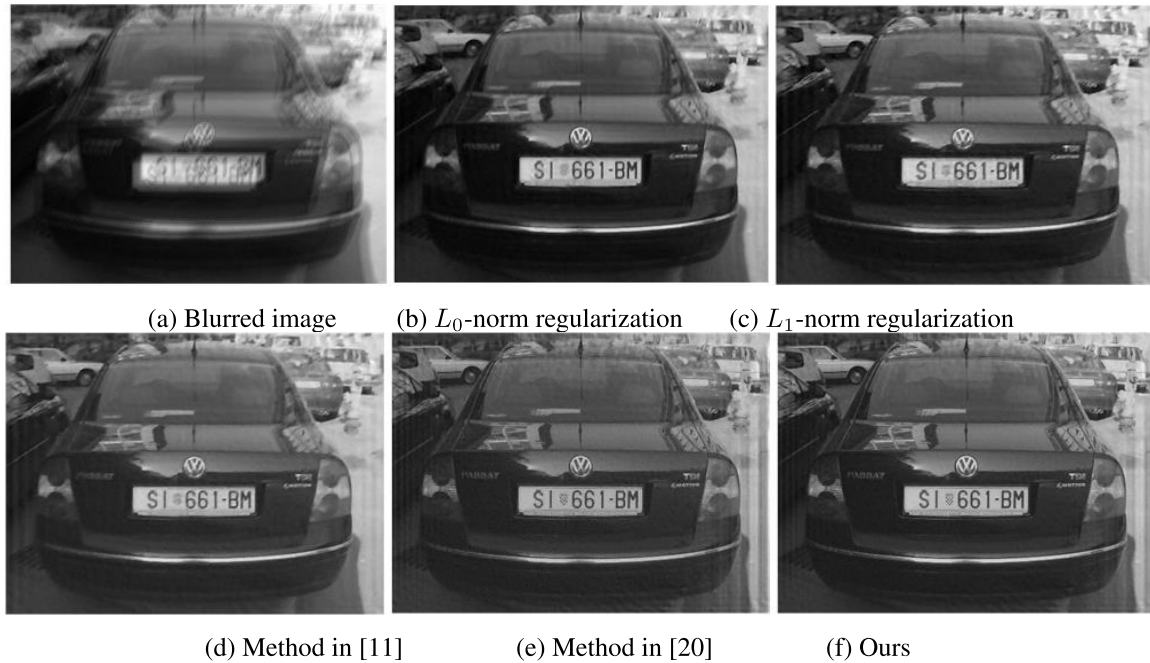(d) Method in [11]   (e) Method in [20]   (f) Ours

FIGURE 12. Deblurring results for H_{M3}.

L_1-norm regularization, method in [11] and method in [20] by 1.68dB, 0.95dB, 0.74dB and 0.63dB, respectively. In terms of SSIM, the proposed method improves these methods by 0.0112, 0.0132, 0.0048 and 0.0016, respectively. In a word, by utilizing L_p-norm based regularization, the proposed method perform better than above methods.

For visual assessment, we show the deblurred results of test images in Figs.7-8 for H_{M1} blur, Figs.9-10 for H_{M2} blur, Figs.11-12 for H_{M3} blur. Our method obtain better results than several previous methods. Taking the license plate images in Fig.11(f) as example, the restored result of our method is visually much better than others, and the license numbers are more easily to be recognized.

IV. CONCLUSION

In this paper, we discuss the statistical distribution characteristics of the license plates. Based on the statistical conclusion that the gradient histogram approximately obeys Hyper-Laplacian distribution, we propose an L_p-norm-based regularization model for license plate deblurring. We introduce alternating direction method of multipliers to solve the model, and demonstrate its performance through a large number of experiments. The proposed model can be regarded as the generalized version of the existing L_0 and L_1 based deblurring method. Moreover, inspired by the variable parameter p in the L_p-norm based regularization model, the regularization term can be optimized through parameter learning. This is the main direction of our future work.

REFERENCES

[1] Z. Liu, R. Li, X. Wang, and P. Shang, "Effects of vehicle restriction policies: Analysis using license plate recognition data in Langfang, China," *Transp. Res. A. Policy Pract.*, vol. 118, pp. 89–103, Dec. 2018.

[2] C. Gou, K. Wang, Y. Yao, and Z. Li, "Vehicle license plate recognition based on extremal regions and restricted Boltzmann machines," *IEEE Trans. Intell. Transp. Syst.*, vol. 17, no. 4, pp. 1096–1107, Apr. 2016.

[3] S. Du, M. Ibrahim, M. Shehata, and W. Badawy, "Automatic license plate recognition (ALPR): A state-of-the-art review," *IEEE Trans. Circuits Syst. Video Technol.*, vol. 23, no. 2, pp. 311–325, Feb. 2013.

[4] Y. Wang, C. Zhao, X. Liu, M. Zhao, and L. Bai, "Fast cartoon-texture decomposition filtering based license plate detection method," *Math. Problems Eng.*, vol. 2018, Jul. 2018, Art. no. 3901906.

[5] A. Perez, M. I. Garcia, M. Nieto, J. L. Pedraza, S. Rodriguez, and J. Zamorano, "Argos: An advanced in-vehicle data recorder on a massively sensorized vehicle for car driver behavior experimentation," *IEEE Trans. Intell. Transp. Syst.*, vol. 11, no. 2, pp. 463–473, Jun. 2010.

[6] J. Jing and Y. Jie, "A recovery algorithm for the details of the low resolution video sequence," in *Proc. 6th Int. Conf. Intell. Inf. Hiding Multimedia Signal Process.*, Oct. 2010, pp. 244–247.

[7] F. Liang, Y. Liu, and G. Yao, "Recognition of blurred license plate of vehicle based on natural image matting," *Proc. SPIE Autom. Target Recognit. Image Anal.*, vol. 7495, Oct. 2009, Art. no. 749527.

[8] P.-L. Hsieh, Y.-M. Liang, and H.-Y.-M. Liao, "Recognition of blurred license plate images," in *Proc. IEEE Int. Workshop Inf. Forensics Secur.*, Dec. 2010, pp. 1–6.

[9] T. Ajanthan, P. Kamalaruban, and R. Rodrigo, "Automatic number plate recognition in low quality videos," in *Proc. IEEE 8th Int. Conf. Ind. Inf. Syst.*, Dec. 2013, pp. 566–571.

[10] J. Pan, Z. Hu, Z. Su, and M.-H. Yang, "Deblurring text images via L0-regularized intensity and gradient prior," in *Proc. IEEE Conf. Comput. Vis. Pattern Recognit.*, Jun. 2014, pp. 2901–2908.

[11] C. Song and X. Lin, "Blurred license plate recognition based on single snapshot from drive recorder," in *Proc. IEEE Int. Conf. Commun. (ICC)*, Jun. 2015, pp. 7108–7113.

[12] W. Zuo, D. Meng, L. Zhang, X. Feng, and D. Zhang, "A generalized iterated shrinkage algorithm for non-convex sparse coding," in *Proc. IEEE Int. Conf. Comput. Vis.*, Dec. 2013, pp. 217–224.

[13] Y. Wang, W. Yin, and J. Zeng, "Global convergence of ADMM in non-convex nonsmooth optimization," Nov. 2015, *arXiv:1511.06324*. [Online]. Available: https://arxiv.org/abs/1511.06324

[14] A. Beck and M. Teboulle, "Fast gradient-based algorithms for constrained total variation image denoising and deblurring problems," *IEEE Trans. Image Process.*, vol. 18, no. 11, pp. 2419–2434, Nov. 2009.

[15] S. Osher, M. Burger, D. Goldfarb, J. Xu, and W. Yin, "An iterative regularization method for total variation-based image restoration," *Multiscale Model. Simul.*, vol. 4, no. 2, pp. 460–489, Jan. 2005.

[16] G.-S. Hsu, J.-C. Chen, and Y.-Z. Chung, "Application-oriented license plate recognition," *IEEE Trans. Veh. Technol.*, vol. 62, no. 2, pp. 552–561, Feb. 2013.

[17] *LPR Database*. Accessed: Jan. 11, 2016. [Online]. Available: http://aolpr.ntust.edu.tw/lab/down-load.html

[18] *ALPD Image Database*. Accessed: Jul. 12, 2016. [Online]. Available: https://sites.google.com/site/samicsemist/about-theteacher/mscthesisdetails

[19] *LP Database*. Accessed: Jun. 15, 2016. [Online]. Available: http://www.emris.fer.hr/projects/LicensePlates/english/bazaslika.zip

[20] Q. Lu, W. Zhou, L. Fang, and H. Li, "Robust blur kernel estimation for license plate images from fast moving vehicles," *IEEE Trans. Image Process.*, vol. 25, no. 5, pp. 2311–2323, May 2016.
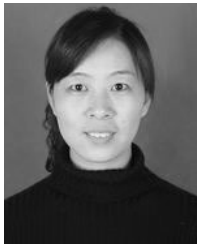
CHENPING ZHAO received the B.S. and M.S. degrees from the School of Mathematics and Statistics, Henan University, Kaifeng, in 2003 and 2006, respectively, and the Ph.D. degree in applied mathematics from the School of Mathematics and Statistics, Xidian University, Xi'an, in 2018. She is currently a Teacher with the School of Mathematical Science, Henan Institute of Science and Technology. Her research interests include variation method and optimization algorithm for image processing.

YINGJUN WANG received the B.S. and M.S. degrees from the School of Computer and Information Engineering, Henan University, Kaifeng, in 2003 and 2006, respectively. He is currently a Teacher with the School of Information Engineering, Henan Institute of Science and Technology. His research interests include embedded system design, machine learning, and image processing.

HONGWEI JIAO received the B.S. degree in mathematics and applied mathematics and the M.S. degree in applied mathematics from Henan Normal University, China, in 2003 and 2006, respectively, and the Ph.D. degree in applied mathematics from Xidian University. He is currently an Associate Professor with the School of Mathematical Sciences, Henan Institute of Science and Technology, China. He has published extensively and holds numerous patents in his research areas. His current research interests include optimization algorithms, system engineering, and optimal control.

JINGBEN YIN received the master's degree from Zhengzhou University, in 2009. He is currently an Associate Professor with the Department of Mathematics, Henan Institute of Science and Technology, China. His research interests include software engineering, computer application, optimization algorithm design, product design, manufacturing information systems, optimization algorithm, nonlinear systems, and optimal control theory. He has published over 30 research monographs.

XUEZHI LI received the B.S. degree in mathematics and applied mathematics from Xinyang Normal University, China, in 1988, the M.S. degree in applied mathematics from the Chinese Academy of Sciences, Beijing, in 1991, and the Ph.D. degree in applied mathematics from the Institute of Mathematics and System Sciences, Chinese Academy of Science, Beijing, in 2001. He is currently the Vice President of Henan Normal University, and a Professor with the College of Mathematics and Information Science, Henan Normal University. His research interests include biological mathematics, distribution parameter system theory, numerical algorithm, and machine learning.

• • •